Immunostimulation by *Lactobacillus kefiri* S-layer proteins with distinct glycosylation patterns requires different lectin partners

Received for publication, April 20, 2020, and in revised form, August 12, 2020 Published, Papers in Press, August 13, 2020, DOI 10.1074/jbc.RA120.013934

Mariano Malamud[1,2,‡], Gustavo J. Cavallero[3,‡], Adriana C. Casabuono[3], Bernd Lepenies[2], María de los Ángeles Serradell[1,*], and Alicia S. Couto[3,*]

From the [1]Cátedra de Microbiología, Departamento de Ciencias Biológicas, Facultad de Ciencias Exactas, Universidad Nacional de La Plata, La Plata, Argentina, the [2]University of Veterinary Medicine Hannover, Immunology Unit & Research Center for Emerging Infections and Zoonoses, Hannover, Germany, and the [3]Universidad de Buenos Aires, Facultad de Ciencias Exactas y Naturales, Departamento de Química Orgánica-Consejo Nacional de Investigaciones Científicas y Técnicas, Centro de Investigación en Hidratos de Carbono, Buenos Aires, Argentina

Edited by Gerald W. Hart

S-layer (glyco)-proteins (SLPs) form a nanostructured envelope that covers the surface of different prokaryotes and show immunomodulatory activity. Previously, we have demonstrated that the S-layer glycoprotein from probiotic *Lactobacillus kefiri* CIDCA 8348 (SLP-8348) is recognized by Mincle (macrophage inducible C-type lectin receptor), and its adjuvanticity depends on the integrity of its glycans. However, the glycan's structure has not been described so far. Herein, we analyze the glycosylation pattern of three SLPs, SLP-8348, SLP-8321, and SLP-5818, and explore how these patterns impact their recognition by C-type lectin receptors and the immunomodulatory effect of the *L. kefiri* SLPs on antigen-presenting cells. High-performance anion-exchange chromatography–pulse amperometric detector performed after β-elimination showed glucose as the major component in the *O*-glycans of the three SLPs; however, some differences in the length of hexose chains were observed. No *N*-glycosylation signals were detected in SLP-8348 and SLP-8321, but SLP-5818 was observed to have two sites carrying complex *N*-glycans based on a site-specific analysis and a glycomic workflow of the permethylated glycans. SLP-8348 was previously shown to enhance LPS-induced activation on both RAW264.7 macrophages and murine bone marrow–derived dendritic cells; we now show that SLP-8321 and SLP-5818 have a similar effect regardless of the differences in their glycosylation patterns. Studies performed with bone marrow–derived dendritic cells from C-type lectin receptor–deficient mice revealed that the immunostimulatory activity of SLP-8321 depends on its recognition by Mincle, whereas SLP-5818's effects are dependent on SignR3 (murine ortholog of human DC-SIGN). These findings encourage further investigation of both the potential application of these SLPs as new adjuvants and the protein glycosylation mechanisms in these bacteria.

Glycosylation is considered the most popular post-translational modification targeting proteins. Although it was assumed that until the mid-1970s that the ability to glycosylate proteins was restricted to eukaryotic cells and archaebacteria (1), nowadays it is known that this post-translational modification is not an exception in eubacteria, although it is early to predict the full extent of prokaryotic glycosylation (2). From the studies performed on eukaryotic cells, it is clear that the presence of glycans affect the expression, localization, and lifetime of numerous proteins, thus affecting its functions as well as several downstream biological events (3).

In eubacteria, protein glycosylation has been extensively studied in pathogens, emphasizing its relevance in virulence and pathogenicity. On the contrary, the nature and function of glycoproteins in nonpathogenic bacteria, including gut commensal species, remains largely unexplored (4). Because interactions between commensal bacteria, intestinal epithelial and immune cells play a crucial role in the maintenance of gut homeostasis, the study of protein glycosylation in gut commensal bacteria has become an expanding field of research because of the importance of the role of gut microbiota in health and disease (5, 6). This is particularly relevant in the case of surface proteins, which act as mediators of several interactions between microorganisms and their host.

The S-layer is a nanostructured proteinaceous envelope constituted by subunits that self-assemble to form a two-dimensional lattice that covers the surface of different species of *Bacteria* and *Archaea* (7). Given their ubiquitous presence, S-layers are considered as the result of evolutionary changes of the microorganisms to survive in harsh environments (8), although there are no reports on common functions for all of them (9). The presence of S-layer has been found in both Gram-negative and Gram-positive bacteria, including pathogenic and nonpathogenic species (10). Regarding the members of the genus *Lactobacillus*, microorganisms commonly retrieved in the gut of different mammalian hosts as well as in fermented foods, the S-layer has been detected in many but not all species (11). Because of their unique self-assembly ability, presenting repetitive identical physicochemical properties down to the subnanometer scale, the S-layer proteins have gained interest in distinct areas of biotechnology, biomimetics, and biomedicine. Indeed, different researchers have been conducted experiments focusing on the application of S-layer proteins

‡These authors contributed equally to this work.
*For correspondence: María de los Ángeles Serradell, maserr@biol.unlp.edu.ar; Alicia Susana Couto, acouto@qo.fcen.uba.ar.

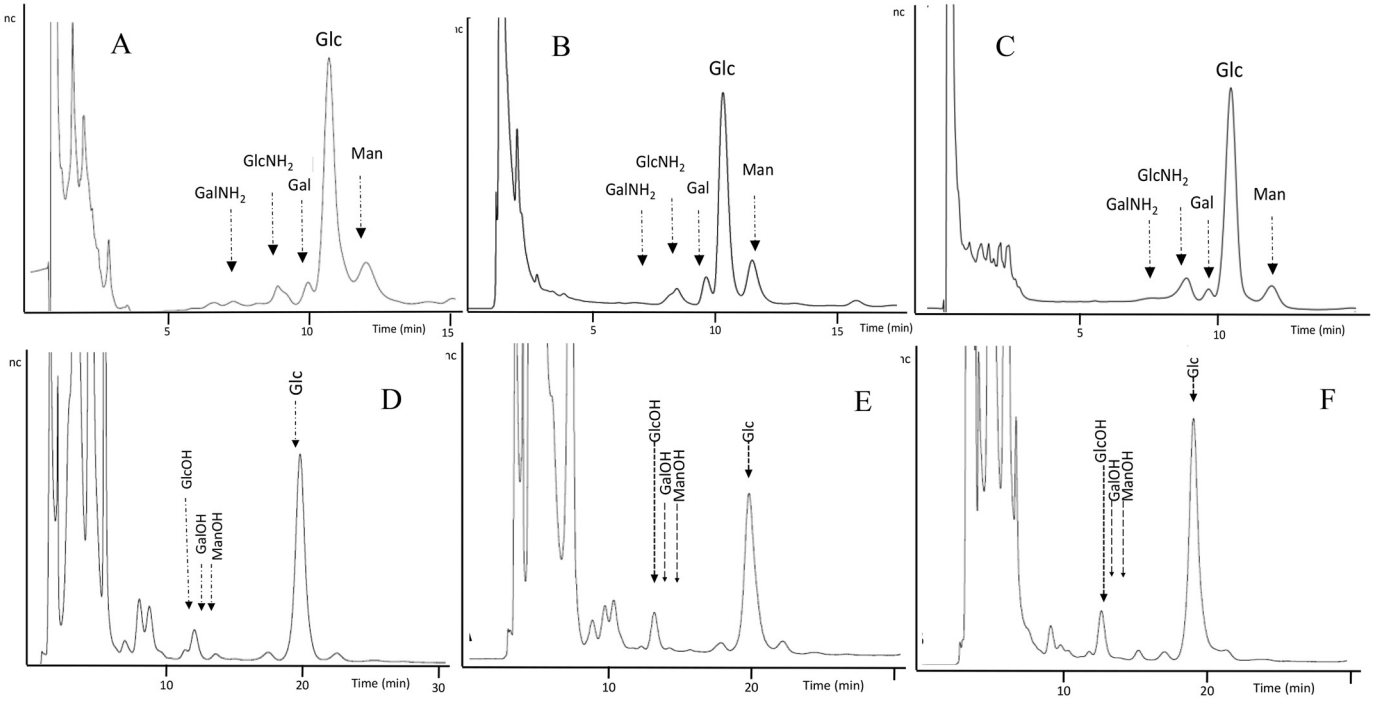

Figure 1. Analysis by HPAEC-PAD of the sugar components of the *O*-glycosidic chains released by reductive β-elimination. *A–C*, neutral monosaccharides released from SLP-5818, SLP-8348, and SLP-8321, respectively. *D–F*, alditols released from SLP-5818, SLP-8348, and SLP-8321, respectively. *Glc*, glucose; *Gal*, galactose; *Man*, mannose; *$GalNH_2$*, galactosamine; *$GlcNH_2$*, glucosamine.

for the development of new antigen/hapten carriers, adjuvants, or vaccination vesicles (11, 12).

After the presence of S-layer proteins in several strains of *Lactobacillus kefiri* formerly isolated from kefir grains and characterized as potentially health-promoting microorganisms was described (13), several studies have been performed in our laboratory to gain knowledge about structural and functional properties of these surface proteins. In particular, the S-layer proteins from *L. kefiri* strains show differences in their amino acid sequences, mainly in the C-terminal region of the polypeptide (14). Moreover, they are part of the small group of glycosylated S-layer proteins reported within the genus *Lactobacillus* (11), and until now, the detailed glycan structures have been described just for the strain *L. kefiri* CIDCA 83111 (15).

Noteworthy, although the S-layer proteins were the first glycoproteins described in prokaryotes, the studies of the role of the glycan residues in the functional properties of these proteins are scarce and are usually focused on some archaea (16) or pathogenic bacteria (17, 18). Regarding the genus *Lactobacillus*, there are some reports describing the involvement of the carbohydrate receptor DC-specific ICAM-3–grabbing nonintegrin (DC-SIGN) in the functional activity of the S-layer proteins from *Lactobacillus acidophilus* NCFM (19), *Lactobacillus plantarum* (20), and *L. kefiri* JCM 5818 (21). In this sense, we have recently demonstrated that the S-layer glycoprotein from *L. kefiri* CIDCA 8348 is able to enhance the LPS-induced response in murine macrophages in a carbohydrate receptor–mediated process (22). Moreover, this SLP improves the OVA-specific cell immune response by triggering maturation of antigen-presenting cells through the recognition of glycan moieties by Mincle (23). However, the structure of its glycans has not been determined so far. Considering all this evidence, in the present work we aim to determine the glycosylation patterns of the S-layer proteins expressed on different strains of *L. kefiri* and to analyze the impact on the immunomodulatory activity on antigen-presenting cells.

Results

Glycan structures of L. kefiri S-layer proteins

We have previously reported the composition and structure of the glycans present in the S-layer protein from *L. kefiri* CIDCA 83111 (15). In this work, glycosylation of the S-layer protein from *L. kefiri* JCM 5818, CIDCA 8348, and CIDCA 8321 (SLP-5818, SLP-8348, and SLP-8321, respectively) were characterized. In this regard, the analysis of both *O*- and *N*-glycans was performed.

O-Glycome analysis

The SDS-PAGE bands corresponding to the purified SLPs of each strain were subjected to reductive β-elimination. Sugar composition was achieved by HPAEC-PAD. For this purpose, the released oligosaccharides were hydrolyzed, and monosaccharides were determined. In the three SLPs examined glucose was detected as the major component (Fig. 1, *A–C*). Also, in the three cases, when an alditol analysis was performed, sorbitol was detected. Taking into account that during the treatment the oligosaccharides linking the peptide are released and the reducing end of the oligosaccharides are reduced by $NaBH_4$ to an alditol, the result indicates that a glucose unit is the linkage between the *O*-linked oligosaccharides and the peptides (Fig. 1, *D–F*).

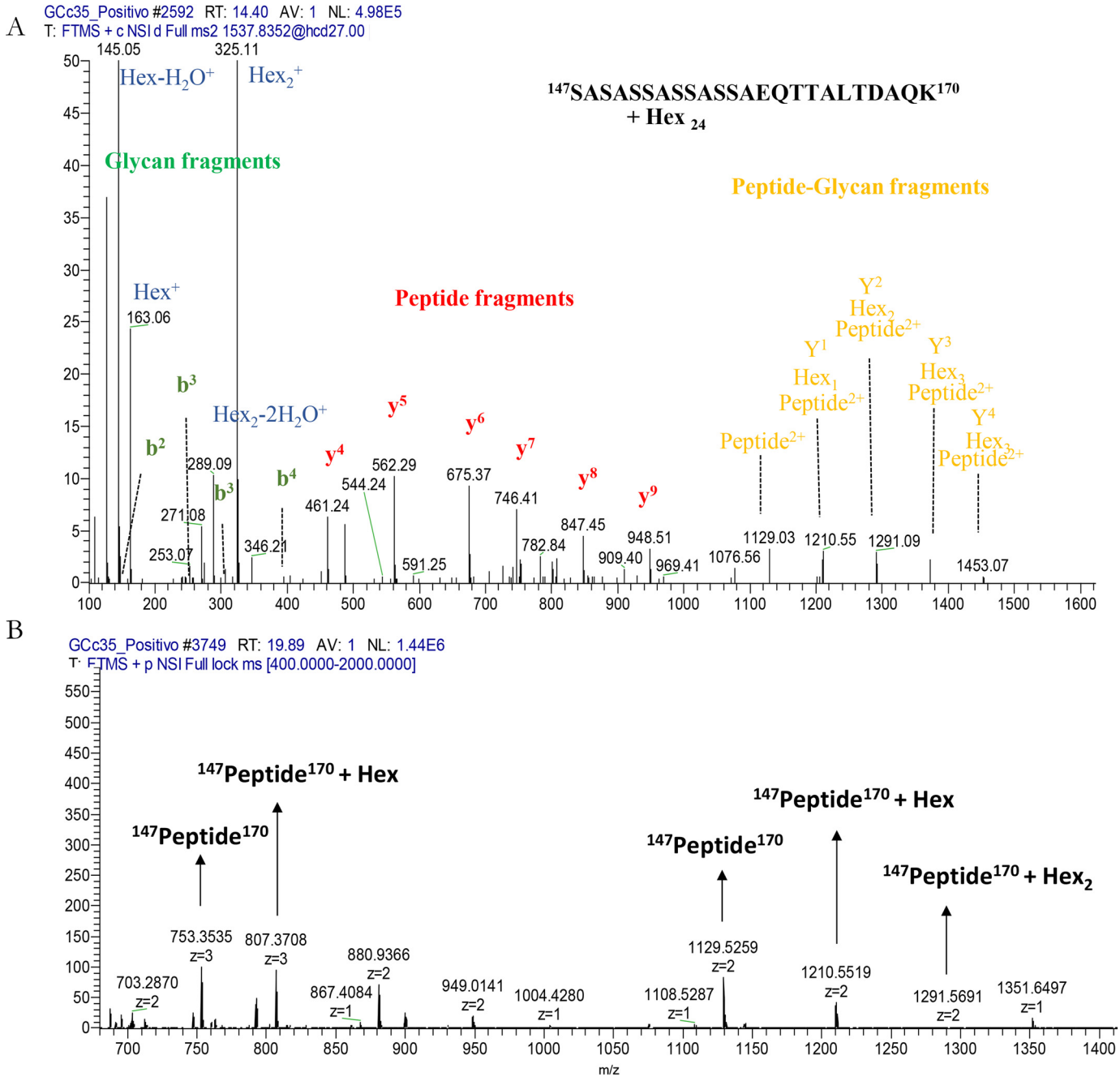

Figure 2. *O*-Glycopeptide analysis by nanoHPLC–ESI–Orbitrap of SLP-5818. *A*, selected MS2 spectra, *m/z* 1537.8352. (y and b peptide fragments and Y glycan-peptide fragments are indicated). *B*, full MS spectrum at retention time 19.89 min showing signals corresponding to 147–170 unmodified peptide and to the same peptide bearing one or two hexose units.

The *O*-glycoproteomic analysis of the SLPs was performed by nanoHPLC–ESI–Orbitrap–HCD. An in-gel trypsin digestion of the purified glycoprotein from each strain was performed followed by a glycopeptide enrichment step using cotton HILIC chromatography. In SLP-5818, the analysis of the extracted ion chromatogram showed a defined region of *O*-glycosylation detected by the extracted ion chromatograms of oxonium ions where up to four hexose units were detected (*m/z* =163.06; 325.11, 487.16, and 649.21). It is known that glycosidic bonds are more labile under the HCD dissociation than peptides. However, notably in this case, a high coverage level of peptide fragmentation was achieved by detecting b and y ions from the glycosylated peptide. Moreover, peptide-glycan fragments (y ions) and the ion corresponding to the naked peptide were also detected (Fig. 2*A*). Deconvolution of the ions allowed the attribution of the signals eluting at retention time between 10 and 14 min to peptide ^{147}SASASSASSASSAEQTTALTDAQK^{170} carrying from 10 to 35 hexoses. Different glycoforms were resolved in the operating conditions of the reverse phase nanoHPLC employed. It is clearly evidenced that the chromatographic elution of *O*-glycopeptides is based on the hydrophilic nature of the attached glycans, therefore on their

Table 1
O-Linked glycosylated peptides of *L. kefiri* CIDCA 5818 S-layer protein

Peptide	m/z M^{+3}			
	Glycoform	Calculated	Expressed	Error
			ppm	
^{147}2256.0353^{170}	Hex_1	807.0367	807.0370	−0.41
	Hex_2	861.0543	861.0551	−0.97
	Hex_3	915.0719	915.0724	−0.58
	Hex_4	969.0895	969.0895	−0.03
	Hex_5	1023.1071	1023.1075	−0.42
	Hex_6	1077.1247	1077.1252	−0.50
	Hex_7	1131.1423	1131.1429	−0.56
	Hex_8	1185.1599	1185.1581	1.49
	Hex_9	1239.1775	1239.1770	0.38
	Hex_{10}	1293.1951	1293.1959	−0.64
	Hex_{11}	1347.2127	1347.2139	−0.92
	Hex_{12}	1401.2303	1401.2311	−0.59
	Hex_{13}	1455.2479	1455.2474	0.32
	Hex_{14}	1509.2655	1509.2646	0.57
	Hex_{15}	1563.2831	1563.2825	0.36
	Hex_{16}	1617.3007	1617.3018	−0.70
	Hex_{17}	1671.3183	1671.3114	4.11
	Hex_{18}	1725.3359	1725.3359	−0.02
	Hex_{19}	1779.3535	1779.3544	−0.52
	Hex_{20}	1833.3711	1833.3687	1.29
	Hex_{21}	1887.3887	1887.3909	−1.18
	Hex_{22}	1941.4063	1941.4103	−2.08
	Hex_{23}	1995.4239	1995.4330	−4.58

decreasing size, from the largest to the smallest one. Interestingly, it was also possible to detect glycosylation from just one hexose unit co-eluting with the nonmodified peptide (Fig. 2*B* and Table 1), indicating that this *O*-glycosylation site is not fully occupied in this protein.

On the other hand, it was interesting to detect in extracted ion chromatograms from both SLP-8321 and SLP-8348 a region where several clusters of ions with charge +4, +5, +6, and +7 corresponding to peptide 125–170 containing the SAS-SASASA motif bearing up to 26 hexose units (Fig. 3, *A* and *B*, and Tables 2 and 3). MS/MS spectrum of the different ions showed b- and y-peptide fragments, confirming the peptide identification (Fig. 3, *C* and *D*).

L. kefiri JCM 5818 N-glycome analysis

Further on, taking into account that the S-layer protein of *L. kefiri* 83111 presented *N*-glycosylation (15), we searched for diagnostic oxonium ions for $HexNAc^+$ (m/z 204.09, 168.07, and 138.05) in the MS/MS spectra. No signals were detected for SLP-8348 and SLP-8321; however, SLP-5818 evidenced the presence of the reporter ions. Therefore, we first tried an affinity-based purification of the SLP of *L. kefiri* JCM 5818 using immobilized wheat germ agglutinin (WGA) to evidence this type of post-translational modification.

Interestingly, although whole protein fraction showed that the purification was not complete (Fig. 4*A*, *lane 2*), the SDS-PAGE profile from the lectin-bound fraction showed a protein band with a molecular mass of 67 kDa in accordance with the reported molecular mass of the SLP-5818 (24, 25) (Fig. 4*A*, *lane 1*). This band was excised, trypsin-digested, and subjected to MS analysis confirming the S-layer protein identity and thus, the presence of *N*-glycosylation in this protein (Table S1 shows protein identification data).

To determine the *N*-glycosylation sites in SLP-5818, we used PNGase F to release the *N*-glycans. It is known that the glycosylated asparagine residue is converted to aspartic acid during the enzymatic reaction (26). As a result, a mass increase of 0.984 Da is obtained in the modified peptide. Based on this strategy, a sample of enriched glycopeptides from SLP-5818 was *N*-deglycosylated using PNGase F and analyzed by nanoHPLC–ESI–Orbitrap. Because spontaneous deamidation might occur, the ratio asparagine/aspartic acid was considered to avoid misassignments (Table S2 shows peptide identification data). Thus, two *N*-glycosylation sites at NVAV**N**^{55}GTNALYTK and at DAALTSL**N**^{457}NTVK were determined. As shown in Fig. 4*B*, MS2 spectrum of peptide NVAV**N**^{55}GTNALYTK showed fragment ion y_9 with a m/z = 982.48 (calc. m/z = 981.50, Δ 0.984 Da) confirming the *N*-glycosylation site at Asn^{55}. In the same way, MS2 spectrum of peptide DAALTSL**N**^{457}NTVK showed y_5-fragment ion m/z = 576.30 (calc. m/z = 575.31, Δ 0.984 Da) evidencing an *N*-glycosidic linkage in Asn^{457} (Fig. 4*C*). Further on, to determine the *N*-glycan structures attached to SLP-5818, we performed an enzymatic hydrolysis of the *N*-oligosaccharides using PNGase F. Glycans were separated, permethylated, and analyzed by nanoHPLC–ESI–Orbitrap. The extracted ion chromatograms corresponding to m/z = 464.24 ($HexNAc\text{-}Hex^+$) and m/z = 189.11 ($dHex^+$) allowed detection of a family of complex permethylated *N*-glycans eluting between real times of 40 and 45 min (Fig. 5*A*). Main structures, m/z, and mass errors are detailed in Table 4. Fig. 6 shows two examples of MS2 spectra of selected ions assigned to two biantennary glycans differing in the composition of one antennae. The permethylated *N*-glycans were also examined using MALDI-TOF MS, and structures corresponding to biantennary species were also detected (Fig. 5*B*).

Stimulation of murine macrophages by L kefiri SLPs

Because we have previously demonstrated that SLP-8348 can enhance LPS-induced activation of antigen-presenting cells (22, 23), we decided to test the ability of SLP-8321 and SLP-5818 to activate murine macrophage, using RAW 264.7 cells as first model. As was previously observed for SLP-8348 (22, 23), the SLP-8321 and SLP-5818 were not able to induce activation of RAW 264.7 cells by themselves. However, respective significant increments in secreted IL-6, as well as in surface expression of CD40 and CD86, were observed for macrophages simultaneously exposed to *Escherichia coli* LPS and *L. kefiri* S-layer glycoproteins compared with LPS-treated cells (Fig. 7, *A* and *B*). To note, no significant differences were observed among the stimulatory activity of strains despite the differences in their glycosylation patterns.

Interaction of SLPs with different C-type lectin receptors

Considering that it has been previously shown for SLP-8348 that the recognition of the glycan residues by a C-type lectin receptor (CLR) is a key event in the immunomodulatory activity of the protein (23), we decided to test the ability of SLP-8321 and SLP-5818 to interact with different CLRs. As shown previously for SLP-8348 (23), SLP-8321 and SLP-5818 bound to the

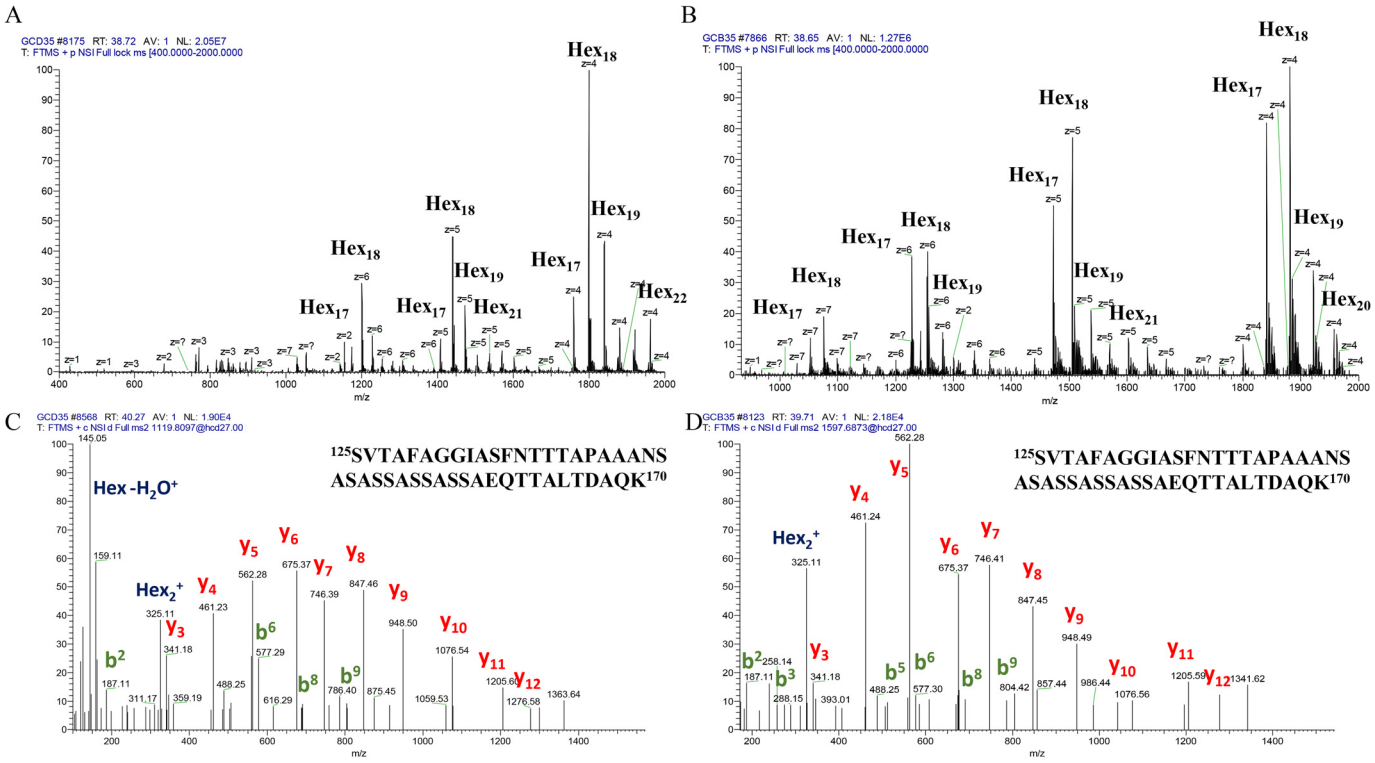

Figure 3. *O*-glycopeptide analysis. *A* and *B*, full MS spectra of SLP-8348 and SLP-8321, respectively, showing glycopeptide families with charge +4, +5, +6 and +7. *C*, MS/MS spectra of ion *m/z* 1119, 8097^{+6} from SLP-8348. *D*, MS/MS spectra of ion *m/z* 1597.6873^{+4} from SLP-8321 (y and b peptide fragments and hexose fragments are indicated).

CLRs DC-SIGN, SingR3, Langerin, and Mincle (Fig. 8*A*). As expected, a reduction of ~70% was observed in the SLP–CLR interactions in the presence of the Ca^{2+}-chelating agent EGTA (Fig. 8*B*).

Activation of BMDC by SLP-8321 and SLP-5818

Regarding the ability of SLP-8321 and SLP-5818 to interact with different CLRs and considering that both glycoproteins enhanced LPS-induced response in murine macrophages, we decided to use BMDCs from C57BL/6 mice as antigen-presenting cells to assess both internalization of SLPs and cell activation. As shown for SLP-8348 (23), we observed that both SLP-8321 and SLP-5818 were internalized by BMDCs in a dose-dependent way (Fig. 9*A*). However, a significant decrease in the uptake of SLP-8321 was observed when BMDCs from Mincle$^{-/-}$ mice were used. On the contrary, the internalization of SLP-5818 was only reduced in BMDCs from SignR3$^{-/-}$ mice and was not affected by the absence of Mincle (Fig. 9*A*).

Following the same methodology previously reported (23), we decided to test the immunomodulatory activity of SLP-8321 and SLP-5818 on BMDCs. Unlike in the case of RAW 264.7 cells, both SLPs were able to induce the maturation of BMDCs because a significant increment in the level of secreted IL-6 and TNFα, as well as in the surface expression of CD40 and CD80, was observed (Fig. 9, *B* and *C*). The same effect was observed when BMDCs were stimulated by a combination of SLPs and LPS. The stimulatory activity of SLP-8321 was lost when BMDCs from Mincle$^{-/-}$ mice were used, whereas SLP-5818 was not able activate BMDCs from SignR3$^{-/-}$ mice (Fig. 9, *B* and *C*).

To further investigate the T-cell stimulatory function of the SLP-activated BMDCs, OVA-treated BMDCs from WT, Mincle$^{-/-}$, SignR3$^{-/-}$, and CARD9$^{-/-}$ were incubated in the presence or absence of SLP-8321 or SLP-5818 with purified T cells from OT-II mice, as was previously performed with SLP-8348 (23). Both SLPs could enhance the OVA-specific T-cell response because a higher IFN-γ secretion as well as higher $CD4^+$ T-cell proliferation were observed upon simultaneous stimulation of WT BMDCs with OVA and SLP-8321 or SLP-5818 compared with OVA-treated antigen-presenting cells (Fig. 10, *A* and *B*). The absence of Mincle abrogated the immunostimulatory activity of SLP-8321, whereas SLP-5818 was not able to enhance $CD4^+$ T-cell response when BMDCs from SignR3$^{-/-}$ mice were used (Fig. 10, *A* and *B*). As was expected, none of the SLPs assessed were able to potentiate $CD4^+$ T-cell activation when assays were performed using BMDC from CARD9$^{-/-}$ mice, a downstream signaling protein of Mincle and SignR3 (27) (Fig. 10, *A* and *B*).

Discussion

Considering the ubiquitous presence of S-layer–carrying microorganisms and the abundance of the S-layer proteins, it is evident that these structures reflect the evolutionary adaptation of the organisms to natural habitats and must have provided them with advantages in specific environmental and ecological conditions (8). Glycosylation is the post-translational modification most frequently found in SLPs, a feature shared with other surface-exposed proteins such as

Table 2
***O*-Linked glycosylated peptides of *L. kefiri* CIDCA 8348 S-layer protein**

Peptide	m/z M^{+3} Glycoform	Calculated	Expressed	Error
				ppm
^{125}4277.0207^{170}	Hex_{22}	1961.5529	1961.5544	−0.78
	Hex_{21}	1921.0397	1921.0396	0.04
	Hex_{20}	1880.5265	1880.5272	−0.39
	Hex_{19}	1840.0133	1840.0141	−0.45
	Hex_{18}	1799.5001	1799.5057	−3.13
	Hex_{17}	1758.9869	1758.9868	0.04
	Hex_{16}	1718.4737	1718.4769	−1.88
	Hex_{15}	1677.9605	1677.9602	0.16
	Hex_{14}	1637.4473	1637.4468	0.29
	Hex_{13}	1596.9341	1596.9348	−0.45
	Hex_{12}	1556.4209	1556.4201	0.50
	Hex_{11}	1515.9077	1515.9086	−0.61
	Hex_{10}	1475.3945	1475.3951	−0.42
	Hex_{9}	1434.8813	1434.8822	−0.64
	Hex_{8}	1394.3681	1394.3696	−1.09
	Hex_{7}	1353.8549	1353.8557	−0.61
	Hex_{6}	1313.3417	1313.3422	−0.40

Table 3
***O*-Linked glycosylated peptides of *L. kefiri* CIDCA 8321 S-layer protein**

Peptide	m/z M^{+3} Glycoform	Calculated	Expressed	Error
				ppm
^{125}4277.0207^{170}	Hex_{22}	1961.5529	1961.5525	0.19
	Hex_{21}	1921.0397	1921.0369	1.44
	Hex_{20}	1880.5265	1880.5252	0.68
	Hex_{19}	1840.0133	1840.0122	0.58
	Hex_{18}	1799.5001	1799.5038	−2.07
	Hex_{17}	1758.9869	1758.9854	0.84
	Hex_{16}	1718.4737	1718.4721	0.92
	Hex_{15}	1677.9605	1677.9615	−0.61
	Hex_{14}	1637.4473	1637.4498	−1.54
	Hex_{13}	1596.9341	1596.9349	−0.52
	Hex_{12}	1556.4209	1556.4187	1.40
	Hex_{11}	1515.9077	1515.9091	−0.94
	Hex_{10}	1475.3945	1475.3958	−0.90
	Hex_{9}	1434.8813	1434.8829	−1.13
	Hex_{8}	1394.3681	1394.3687	−0.45
	Hex_{7}	1353.8549	1353.8516	2.42
	Hex_{6}	1313.3417	1313.3427	−0.78
	Hex_{5}	1272.8285	1272.8290	−0.41
	Hex_{4}	1232.3153	1232.3162	−0.75

flagellin and pilin. Within the genus *Lactobacillus*, the glycoprotein nature of the S-layer proteins has been reported for strains of *Lactobacillus buchneri* (28, 29), *L. plantarum* 41021/252 (28), *L. acidophilus* NCFM (19), *L. acidophilus* ATCC 4356 (30), and several strains of *L. kefiri* (14, 24). In this last species, we have previously described the composition and structure of the *O*- and *N*-glycans present in the SLP of the strain *L. kefiri* CIDCA 83111 (15). Herein, we show that SLP-5818 also presents *O*- and *N*-glycosylated chains. In this case, peptide 147–170 is *O*-glycosylated in average with eight hexose units, but at difference with the SLP from *L. kefiri* CIDCA 83111, is not decorated with galacturonic acid (15). Regarding *N*-glycans, both SLP-5818 and SLP-83111 present two *N*-glycosylation carrying bianntenary chains.

On the other hand, SLP-8321 and SLP-8348 show 100% of homology at primary sequence level (14), and although they present six potential *N*-glycosylation sites, no evidence of bearing *N*-glycans was found. On the contrary, *O*-glycosidic chains constituted by 4–12 glucose units were detected in both SLPs.

Interstrain differences in the glycosylation patterns of SLP were also seen some years ago in *Thermoanaerobacter thermohydrosulfuricus* and *Thermoanaerobacterium thermosaccharolyticum* (31). Moreover, in *Clostridium difficile* the presence of a glycosylated SLP was only demonstrated in the strain Ox247, which encodes a putative glycosylation locus (18), whereas normally most *C. difficile* strains do not possess a glycosylated S-layer (32). On the other hand, Anzengruber *et al.* (29) reported that SlpB from *L. buchneri* CD034, SlpN from *L. buchneri* NRRL B-30929, and *L. buchneri* SlpB from 41021/251 showed identical *O*-glycans consisting of on average seven glucoses at four serine residues within the sequence ^{152}SASSAS^{157} without any evidence of the presence of *N*-glycosidic chains in those SLP. In this sense, SLP-8321 and SLP-8348 show a higher similarity to the SLPs from *L. buchneri* strains than SLP-83111 and SLP-5818. Further studies are needed to elucidate the mechanisms through which the glycan chains are coupled to the peptide backbone in these surface proteins.

As surface-exposed structures, the SLPs could be a key mediator between bacteria and host immune system contributing to the shaping of the immunological response to pathogenic, commensal, and probiotic microorganisms. By using murine macrophages RAW 264.7 cells as a model, we have demonstrated that despite the differences between glycosylation patterns of SLP-8321 and SLP-5818, both proteins are able to enhance LPS-induced cell activation (Fig. 7), similarly to previously demonstrated for SLP-8348 (22). These results suggest that *O*-glycans present in these three mentioned *L. kefiri* SLPs could be responsible, at least in part, of their immunostimulatory ability.

On the other hand, as previously described with SLP-8348 (23), the assays using BMDCs from Mincle$^{-/-}$ and SignR3$^{-/-}$ mice allowed us to determine that the internalization of SLP-8321 and SLP-5818, as well as their ability to activate BMDCs, was mainly mediated by Mincle and SignR3 (the murine ortholog of human DC-SIGN), respectively (Fig. 9), which could be expected considering the differences in the glycosidic moieties present in those proteins. Moreover, the incubation of BMDCs with SLPs from different *L. kefiri* strains leading to the enhancement of activation of OVA-specific CD4^{+} T cells from OT-II mice, is also dependent on the presence of Mincle and SignR3 for SLP-8321 and SLP-5818, respectively (Fig. 10). Some years ago, a pioneering work performed using a SlpA-knockout mutant *L. acidophilus* NFCM revealed that recognition of SlpA by DC-SIGN in presence of LPS induce an anti-inflammatory response in human monocyte-derived dendritic cells (19), suggesting the involvement of glycans in the immunomodulatory properties of SLPs. More recently, it was demonstrated that *L. acidophilus* NCK2187, a strain that solely expresses SlpA, and its purified SlpA binds to SignR3 to trigger regulatory signals that result in mitigation of experimental colitis, maintenance of healthy gastrointestinal microbiota, and mice protection (33). In addition, the ability of DC-SIGN to recognize the SLP-5818 was recently suggested by Prado Acosta *et al.* (21), which agrees with our findings. However, the role of glycan residues, as well as the CLR involved in the internalization and immunostimulatory activity of SLP-5818, had not been reported so far. On the contrary, it is not surprising

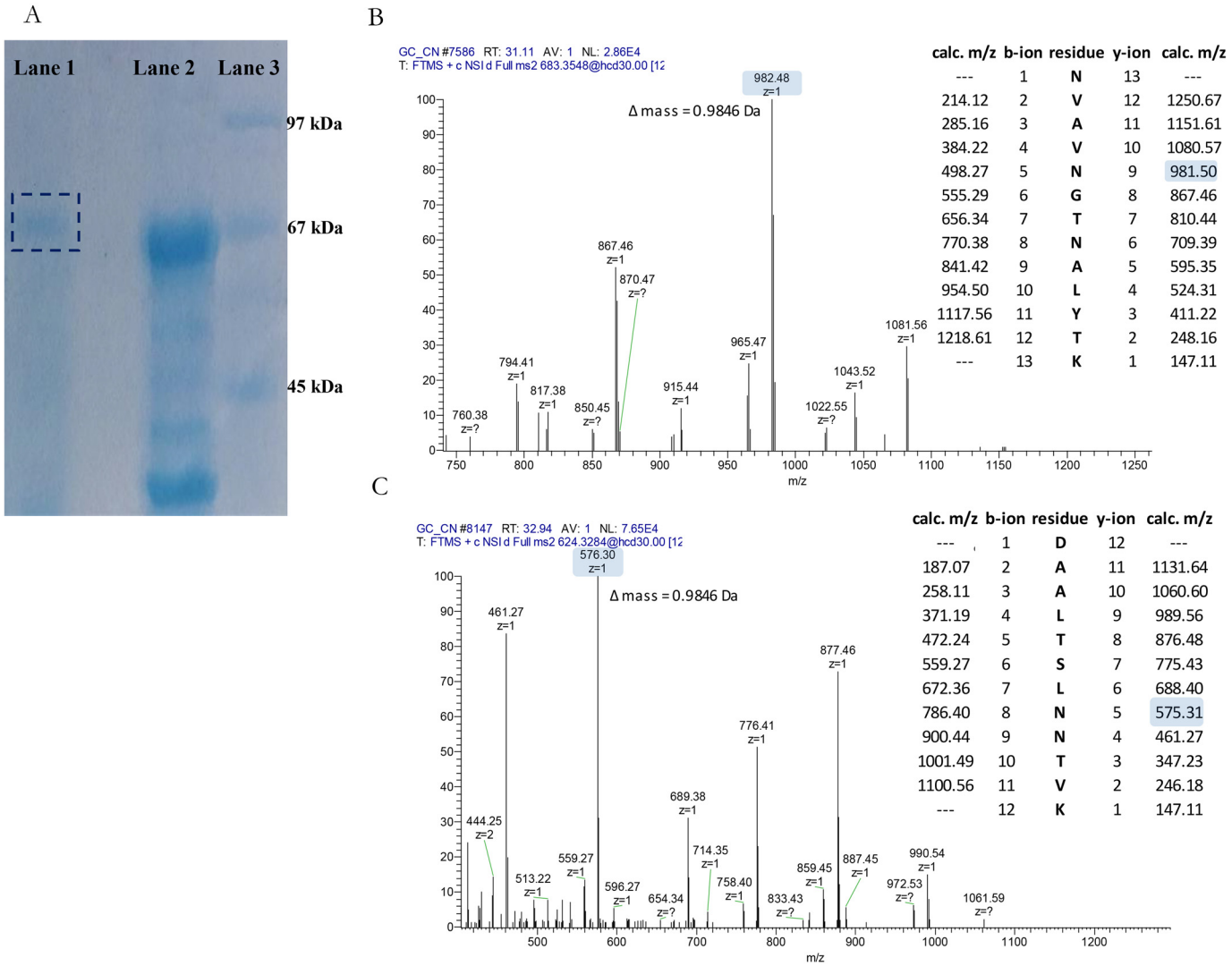

Figure 4. *N*-Glycosylation analysis of SLP-5818. *A*, WGA–Sepharose analysis. *Lane 1*, lectin-bound glycoprotein; *lane 2*, SLP extract; *lane 3*, molecular mass markers. *B* and *C*, MS2 spectra of enzymatically deglycosylated peptides: peptide 51–63 (*B*) and peptide 450-461 (*C*), containing the 0.9846-Da mass increase derived from Asn/Asp conversion. Differences between the *in silico* digested peptides (b and y ions in the *inset*) and the experimental masses are highlighted in *blue*.

that Mincle, the CLR responsible for the recognition and adjuvanticity of the SLP-8348 (23), mediates the immunostimulatory effect of SLP-8321 on BMDCs because both glycoproteins present not only the same amino acid sequence (14) but also the same *O*-glycans. It is known that Mincle recognizes diverse sugar-containing ligands including trehalose dimycolate glycolipid from mycobacteria; mannose-, glucose-, or fucose-containing glycoconjugates; and Lewis antigen from *Helicobacter pylori* LPS (34). To note, it was recently reported that Mincle also recognize the *O*-linked oligosaccharides of the SLP from the Gram-negative oral pathogen *Tannerella forsythia* and that interaction induces both pro- and anti-inflammatory cytokine secretion in macrophages (17).

To resume, despite the differences in glycosylation patterns, as well as the involvement of different CLRs, the glycosylated SLPs from distinct *L. kefiri* strains can induce activation of antigen-presenting cells through the recognition of their glycans. Taken together, these findings encourage us to further investigate the potential application of these surface proteins derived from probiotic bacteria to the development of new adjuvants or carrier for vaccine antigens, as well as to get deeper insight into the protein glycosylation mechanisms in these bacteria.

Experimental procedures

Bacterial strains and culture conditions

L. kefiri CIDCA 8321 and 8348 belonging to the collection of the CIDCA (35) and *L. kefiri* JCM 5818 were used. Bacteria were cultured in deMan–Rogosa–Sharpe broth (DIFCO, Detroit) at 37 °C for 48 h, under aerobic conditions.

S-layer protein extraction

Extraction from bacterial cells at stationary phase was performed using 5 M LiCl as described previously (22). The samples were centrifuged, and the protein concentration in the

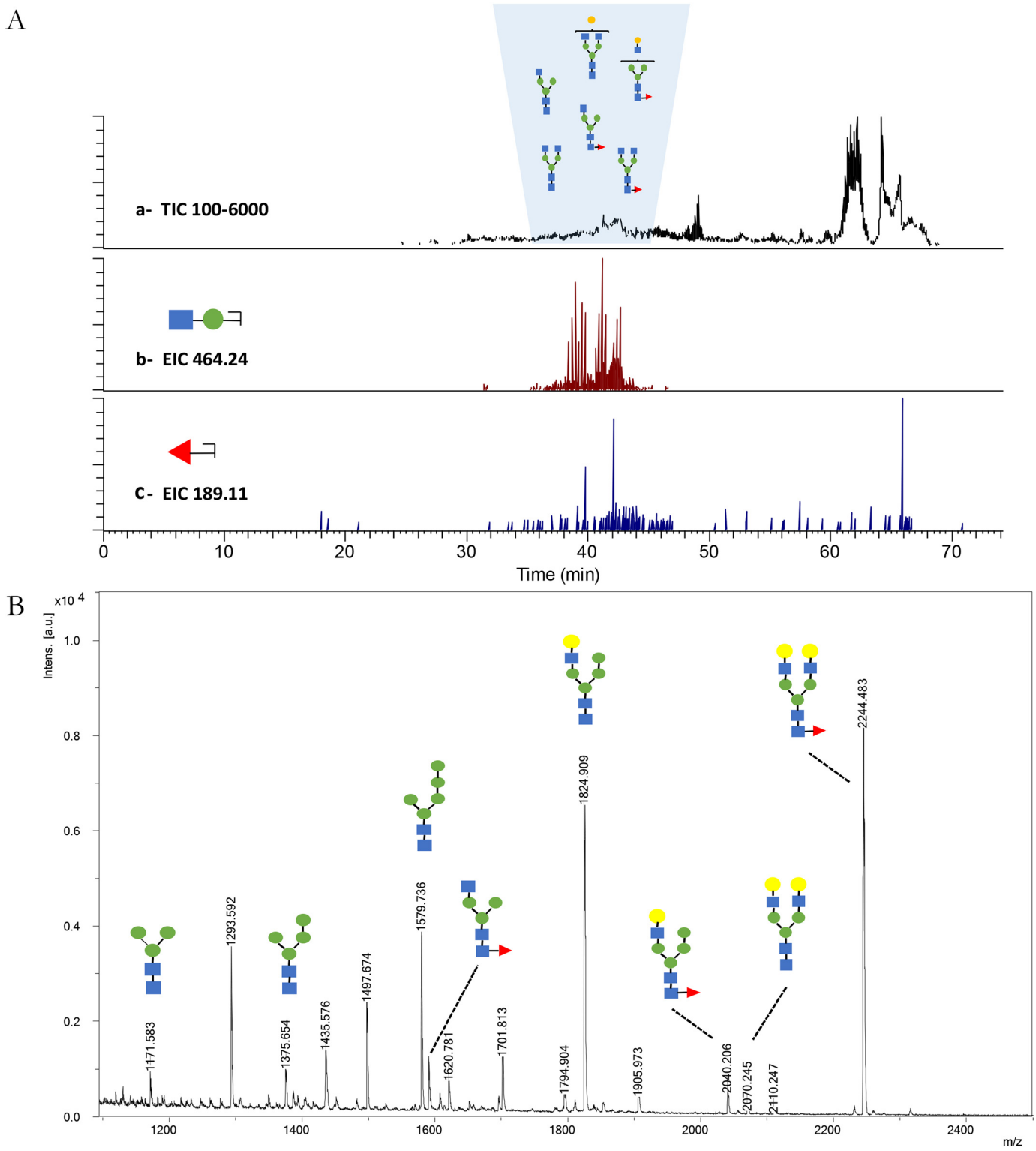

Figure 5. *A*, nanoHPLC–ESI–Orbitrap analysis of permethylated *N*-glycans. *Panel a*, total ion current chromatogram. *Panels b* and *c*, extracted ion chromatograms of permethylated oxonium ions: *m/z* 464.24 (*panel b*, Hex-HexNAc oxonium ion) and *m/z* 189.11 (*panel c*, dHex oxonium ion). *Red triangles*, dHex; *green* and *yellow circles*, Hex; *blue squares*, HexNAc. *B*, MALDI-TOF MS spectrum of permethylated *N*-glycans.

supernatant was determined according to Bradford. The homogeneity of the protein extracts was tested by SDS-PAGE and stained with Coomassie Blue (36). S-layer proteins were filtrated through a membrane of 0.22-μm pore diameter for cellular stimulation assays.

Composition and structure of glycan moieties

Lectin-based N-glycoprotein purification

The enrichment of glycoproteins was performed using WGA lectin affinity chromatography. Briefly, 1 ml of WGA–Sepharose (Sigma) was loaded onto a 5-ml column. Prior to sample

Table 4
Summary of main *N*-glycan structures determined in *L. kefiri* JCM 5818 surface layer protein

N-Glycan	$[M + H]^{2+}$ *m/z*		
	Calculated	Observed	Error
			ppm
HexNAc4-He× 5-dHex	1111.5749	1111.5746	0.3
HexNAc4-He× 4-dHex	1009.525	1009.5243	0.7
HexNAc3-He× 4-dHex	886.96185	886.962	0.2
HexNAc4-He× 3-dHex	907.4751	907.4769	2.0
HexNAc4-Hex5	1024.5303	1024.5303	0.0
HexNAc4-Hex4	922.4804	922.4775	3.1

purification, the stationary phase was equilibrated with 20 mM Tris, pH 7.5, 0.5M NaCl, 1 mM $CaCl_2$, 1 mM $MgCl_2$. Then 50 μl of protein sample was loaded using the latter buffer solution. Nonglycosylated proteins were washed using 20 mM Tris, pH 7.5, containing 1 M NaCl, 1 mM $CaCl_2$, 1 mM $MgCl_2$. Finally, the retained glycoproteins were eluted using the above buffer solution containing 0.5 M *N*-acetyl-D-glucosamine. The glycoprotein fraction was dialyzed against ultrapure water using Spectra/Por® (Repligen) molecular porous membrane tubing with a cutoff of 3.5 kDa. The lectin-based purification was monitored by SDS-PAGE and stained with Colloidal Coomassie Blue.

Release of N-glycosidic chains by PNGase F treatment

The SDS-PAGE S-layer glycoprotein band was cut out from the gel, frozen for 3 h and successively washed with (*a*) acetonitrile, (*b*) 20 mM $NaHCO_3$, pH 7, and (*c*) acetonitrile. The gel pieces were dried, and the *N*-glycans were released by incubation with PNGase F (20 milliunits) (New England Biolabs, Inc., Beverly, MA) overnight at 37 °C in 20 mM $NaHCO_3$, pH 7. The gel pieces were thoroughly washed, and the supernatants were separated and filtered through an Ultrafree McFilter (M_r 5000), dried, resuspended in 0.1% (v/v) formic acid (20 μl), and left at room temperature for 40 min. Finally, the glycans were dried and suspended in water.

Glycoprotein digestion

The protein band corresponding to the S-layer glycoproteins were cut out from the gel and washed with acetonitrile. The gel pieces were reduced with 10 mM DTT in 50 mM NH_4HCO_3 at 55 °C for 30 min. They were further washed with acetonitrile and alkylated with 55 mM iodoacetamide in 50 mM NH_4HCO_3 for 20 min at room temperature in darkness. After washing the gel pieces with 50 mM NH_4HCO_3 for 10 min and with acetonitrile for 5 min, they were dried in a SpeedVac and submitted to digestion with 20 ng/μl trypsin (Sigma) in 40 mM NH_4HCO_3, 9% acetonitrile at 37 °C overnight. Afterward, the supernatants were separated and dried.

In gel-reductive β-elimination and sugar analysis

O-Linked glycans were released from each SDS-PAGE band of the S-layer glycoproteins using 0.05 M NaOH, 1 M $NaBH_4$ and incubated overnight at 50 °C. The solution was separated, and acetic acid was added until pH 7 followed by repeated evaporation with methanol. The sample was dissolved in water, desalted in a Dowex 50 W (H^+) (Fluka) column, and dried in SpeedVac. The β-eliminated samples were further hydrolyzed in 2 N TFA for 4 h at 100 °C. The acid was eliminated by evaporation, and the hydrolysates were resuspended in water for HPAEC-PAD. Analysis was performed using a DX-500 Dionex BioLC system (Dionex Corp.). For neutral and amino sugars, a CarboPac PA20 with the corresponding guard column was used. Isocratic separations were achieved with 18 mM NaOH, and the flow rate was set to 0.4 ml/min. For alditols, a CarboPac MA 1 column was used with a 0.4 M NaOH isocratic program and a flow rate of 0.4 ml/min.

Permethylation of released oligosaccharides

After PNGase digestion, the oligosaccharides were methylated with NaOH in DMSO followed by addition of CH_3I as described (37).

Glycopeptide enrichment

Sample purification and glycopeptide enrichment was achieved by solid-phase extraction cotton HILIC microtips as described (38). Briefly, HILIC microtips were equilibrated with three volumes of 85% ACN. Dried sample was resuspended in 85% acetonitrile. Prior to SPE clean-up step, samples were loaded onto the stationary phase by aspirating and dispensing the protein mixture. The peptides were washed off from the column with 85% ACN, 0.5% TFA, and the retained glycopeptides were eluted using water. The glycopeptide fraction was freeze-dried and stored at −20 °C until MS analysis.

MS analysis

The enriched glycopeptide mixtures were re-suspended in 50% acetonitrile, 1% formic acid/water (1:1). The digests were analyzed in a nanoLC 1000 coupled to an EASY-Spray Q Exactive mass spectrometer (Thermo Scientific) with a HCD and an Orbitrap analyzer. An EASY-Spray PepMap RSLC C18 column (50 μm × 150 mm; particle size, 2.0 μm; pore size, 100 Å) at 40 °C was used. Separation was achieved with a linear gradient from 5% to 35% solvent B developed in 75 min, at a flow of 300 nl/min (mobile phase A: water, 0.1% formic acid; mobile phase B: acetonitrile, 0.1% formic acid). Injection volume was 2 μl. Spray voltage was 3.5 kV (+) or 3.0 kV (−). A full-scan survey MS experiment was performed (*m/z* range, 400–2000; automatic gain control target, 3×10^6; maximum IT, 200 ms; resolution at 400 *m/z,* 70,000). The data-dependent MS2 method was set to the centroid mode; resolution was 17,500; maximum IT was 50 ms; automatic gain control target was 105; the fragment included the top 15 peaks in each cycle; and normalized collision energy was 27. For the analysis of permethylated oligosaccharides, HPLC separation was achieved with a linear gradient of solvent B from 5% to 60% developed in 75 min (flow, 300 nl/min; solvent A was water, 0.1% formic acid; solvent B was ACN, 0.1% formic acid; injection volume, 5 μl).

MALDI-TOF-MS analysis

Measurements were performed using an Ultraflex II TOF/TOF mass spectrometer (Bruker Daltonics GmbH, Bremen, Germany) equipped with a solid-state laser (λ = 355 nm). The system

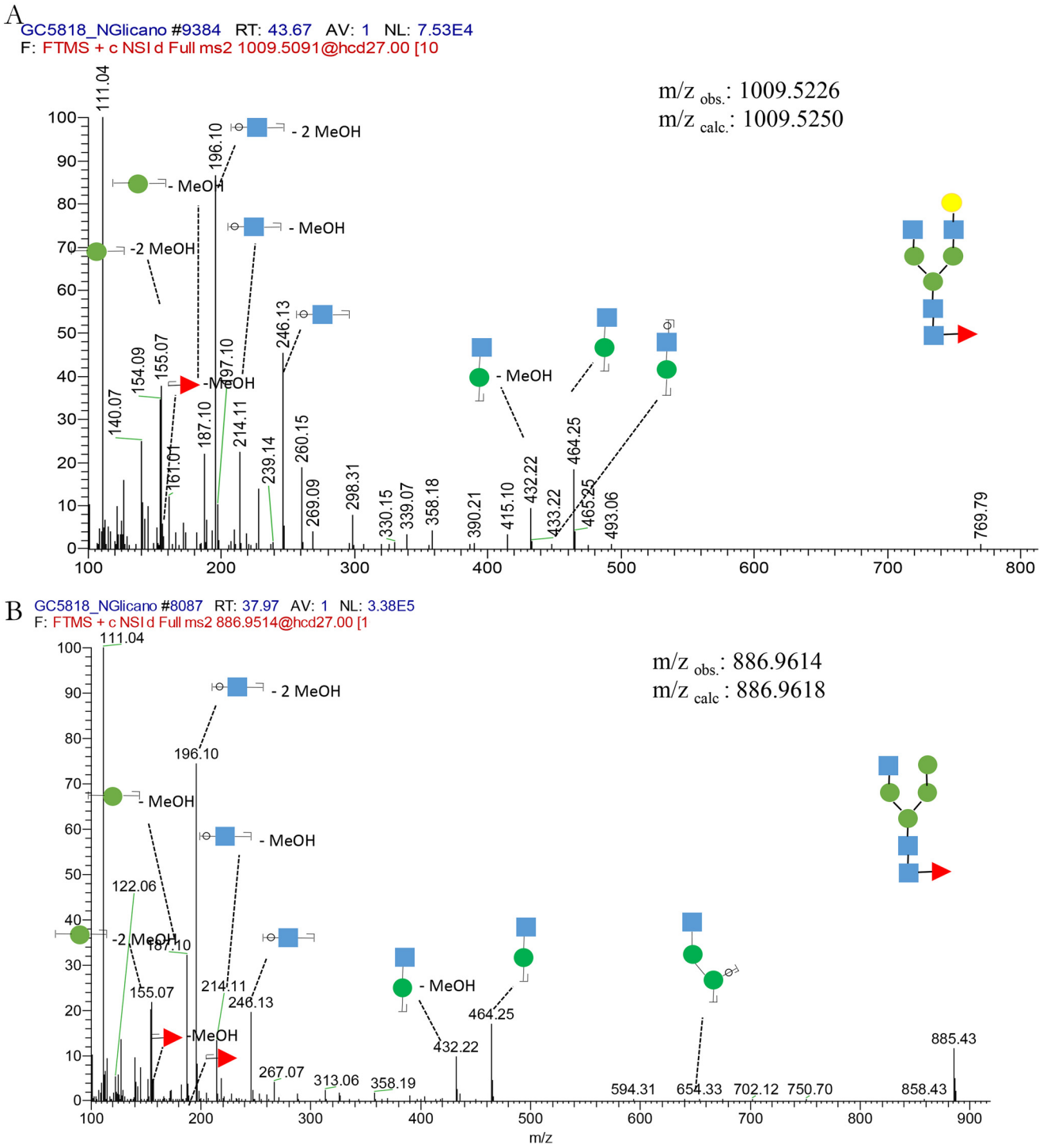

Figure 6. Selected MS2 spectra of permethylated *N*-glycans detected by nanoHPLC–ESI–Orbitrap analysis. *A*, *m/z* 1009.5226. *B*, *m/z* 886.9614. *Red triangles*, dHex; *green* and *yellow circles*, Hex; *blue squares*, HexNAc.

was operated by the Flexcontrol 3.3 package (Bruker Daltonics GmbsH, Bremen, Germany) using gentisic acid as matrix.

Data analysis

Proteome Discoverer 2.1 (Thermo Scientific) assisted protein identification. The mass tolerances for MS and MS/MS were 10 ppm and 0.02 Da, respectively. Missed cleavages allowed for tryptic digestion was 1. Carbamidomethylation of cysteine residues was set as static modification and oxidation of methionine as dynamic modification. For *N*-glycosite analysis, conversion of asparagine to aspartic acid was included as dynamic modification. Precursor mass tolerance was 10 ppm, and fragment mass tolerance was 20 ppm. Confident identification for peptides was set to a score of >100.

Glycopeptide search was performed with MaxQuant version 1.6.5, Byonic™ from ProteinMetrics, Proteome Discoverer 2.2

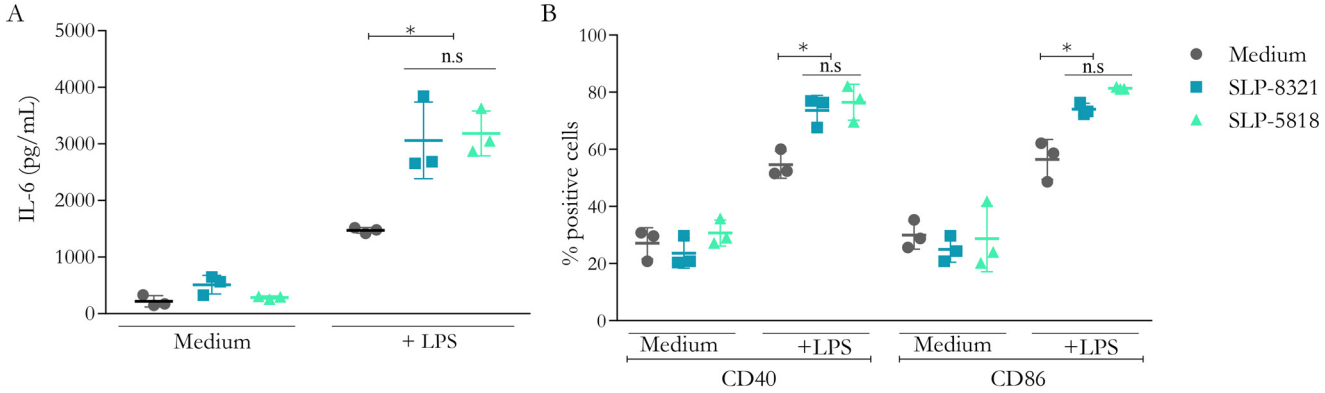

Figure 7. Modulation of LPS-induced maturation of macrophages by *L. kefiri* SLP-8321 and SLP-5818. *A*, IL-6 concentration (pg/ml) by capture ELISA in the supernatant of the murine RAW 264.7 cultures after 24 h of stimulation. *B*, percentage of CD40+ and CD86+ RAW 264.7 cells after 24 h of stimulation. A representative figure of three independent experiments is shown (±S.D., indicated by *error bars*). *, $P < 0.05$; *n.s.*, not significant.

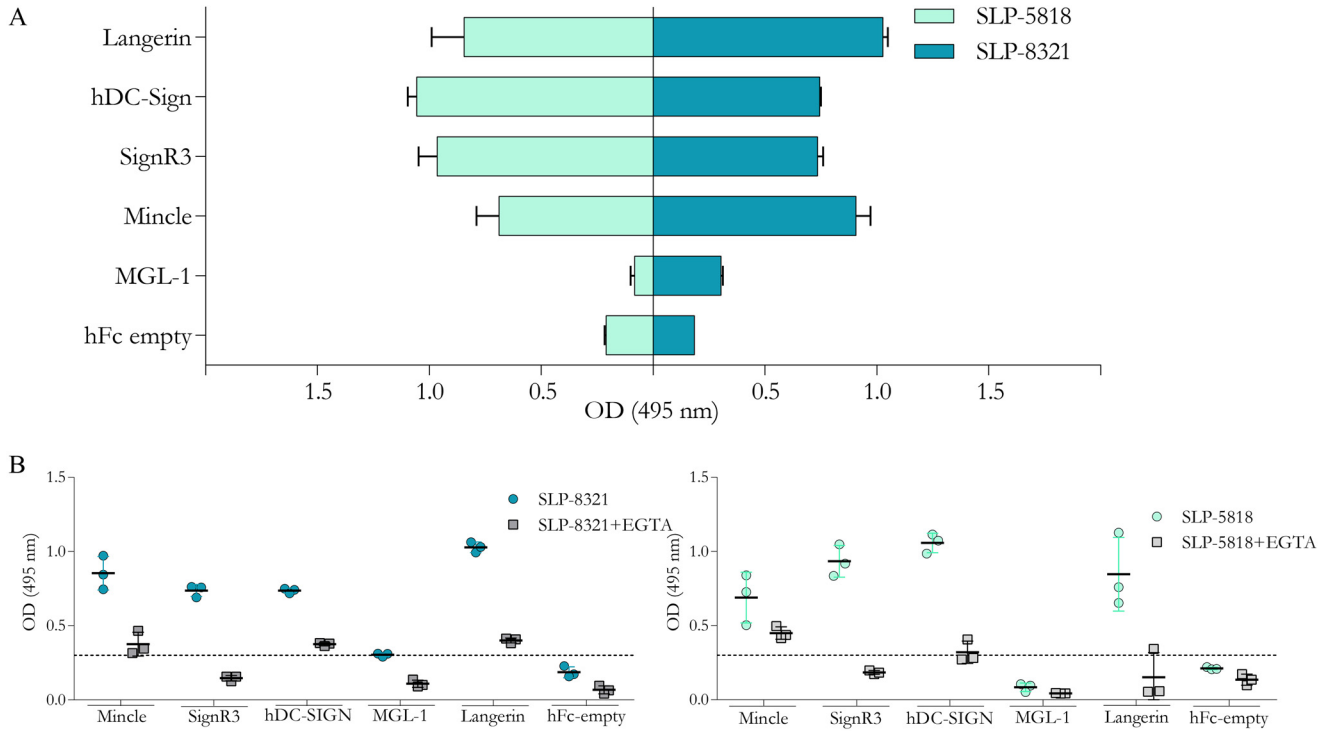

Figure 8. C-type lectin receptor recognition of SLP-8321 and SLP-5818. *A*, reactivity of CLR–hFc fusion proteins on SLP was evaluated by an ELISA type assay (using the same experimental model as in Ref. 23). *B*, inhibition assays were performed using EGTA, a Ca^{2+}-chelating agent. These are representative figures of three independent experiments (±S.D., indicated by *error bars*).

and using a semiautomatic homemade software (A0A1C3S3I4 S-layer protein OS=Lactobacillus kefiri OX = 33962 GN= S-layer A0A1C3S3T6 S-layer protein OS=Lactobacillus kefiri OX = 33962 GN=S-layer). All glycopeptides identifications from both searches were manually curated. MS-Convert Tool (from ProteoWizard platform tools) converted raw data from enriched glycopeptides into text files for manual annotation. Deconvolution was assisted by Xtract on Thermo Xcalibur 3.0.63.

C-type lectin receptor recognition of S-layer proteins

The CLR reactivity on S-layer proteins from *L. kefiri* CIDCA 8321 (SLP-8321) and *L. kefiri* JCM 5818 (SLP-5818) was evaluated by an ELISA type assay as described previously (23, 39). A half-area microplate (Greiner Bio-One GmbH, Frickenhausen, Germany) was coated with 0.25 μg of SLP per well for 16 h at 4 °C and blocked with 1% BSA (Thermo Fisher Scientific, Darmstadt, Germany) for 2 h at room temperature. Then 0.25 μg of each CLR–hFc fusion protein in lectin-binding buffer (50 mM HEPES, 5 mM $MgCl_2$, and 5 mM $CaCl_2$) was added and incubated for 1 h at room temperature. For inhibition assays, CLR–hFc fusion proteins were preincubated with 5 mM of EGTA (Sigma–Aldrich). After washes, horseradish peroxidase–conjugated anti-human IgG anti-body (Dianova) was added to each well for 1 h at room temperature. Finally, the plates were incubated with chromogenic substrate (o-phenylenediamine dihydrochloride substrate tablet (Thermo Fisher Scientific), 24 mM citrate buffer, 0.04% H_2O_2, 50 mM phosphate buffer in H_2O). The reaction was stopped with 2.0 M sulfuric acid and the product was read at

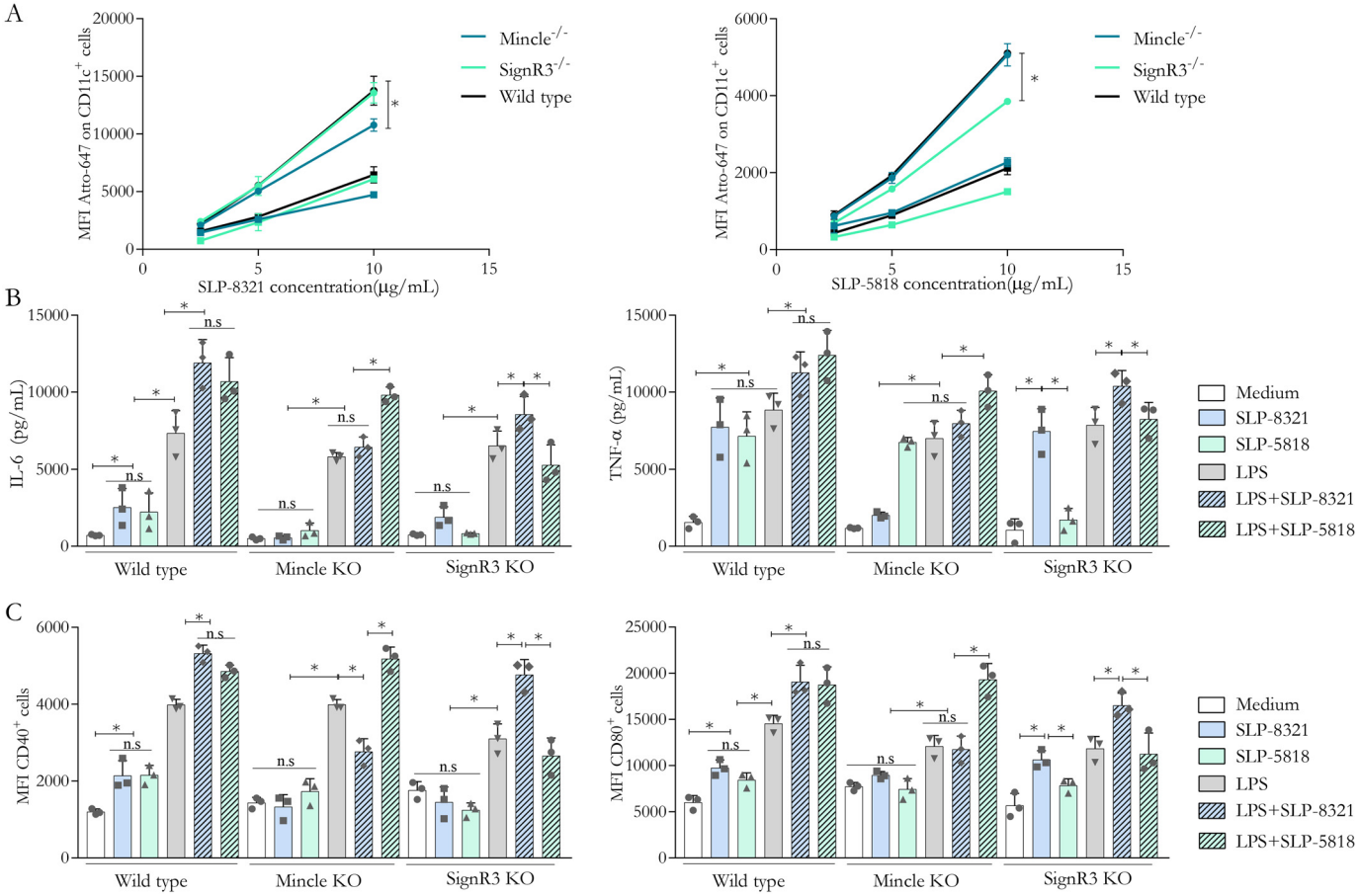

Figure 9. SLP-8321 and SLP-5818 are recognized by specific CLRs expressed on BMDCs. *A*, binding (4 °C, *squares*) and internalization (37 °C, *circles*) of Atto 647N–labeled SLP at different concentrations on CD11c+ cells from C57BL/6 and CLR-deficient mice. *B*, level of IL-6 and TNFα in culture supernatant of BMDCs from C57BL/6 and CLR-deficient mice after stimulation with SLPs, LPS, or the combination of both for 24 h. *C*, cell-surface expression of CD40 and CD86 on CD11c+ cells from C57BL/6 and CLR-deficient mice after stimulation with SLPs, LPS, or the combination of both for 24 h. A representative figure of three independent experiments is shown, following the same experimental lines described in Ref. 23 (±S.D., indicated by *error bars*). *, $P < 0.05$; *n.s.*, not significant; *KO*, knockout.

495 nm using a Multiskan Go microplate spectrophotometer (Thermo Fisher Scientific).

Mice

The source of the CLR- and CARD9-deficient mice was described previously (40–42). Mincle$^{-/-}$, SignR3$^{-/-}$ and CARD9$^{-/-}$ mice were backcrossed on C57BL/6 background over 10 generations in the animal facility of the Federal Institute for Risk Assessment (Berlin, Germany). All mouse lines (including WT and C57BL/6-Tg (TcraTcrb)425Cbn/J (OT-II) mice) were kept in the animal house of the University of Veterinary Medicine (Hannover, Germany) with water and food supplied *ad libitum*. Mice were sacrificed for the isolation of spleen cells (OT-II transgenic mice) or the preparation of bone marrow for BMDC generation (Mincle$^{-/-}$, CARD9$^{-/-}$, SignR3$^{-/-}$, and WT mice). Sacrificing of mice for scientific purposes was approved by the Animal Welfare Officers of the University of Veterinary Medicine Hannover (AZ 02.05.2016).

Cell cultures

The monocyte/macrophage murine cell line RAW 264.7 was cultured in Dulbecco's modified Eagle's medium supplemented with: 10% (v/v) heat-inactivated (30 min/60 °C) fetal bovine serum (FBS), 1% (v/v) nonessential amino acids and 1% (v/v) penicillin-streptomycin solution (100 units/ml penicillin G, 100 g/ml streptomycin). All cell culture reagents were from GIBCO BRL Life Technologies (Rockville, MD).

BMDCs were generated from C57BL/6 WT, Mincle $^{-/-}$, CARD9$^{-/-}$, or SignR3 $^{-/-}$ bone marrow precursors (2.5×10^5 cells/ml) that were plated in complete culture medium (Iscove's modified Dulbecco's medium supplemented with 2 mM glutamine, 10% (v/v) FBS, 100 units/ml penicillin, and 100 μg/ml streptomycin) supplemented with a granulocyte/macrophage colony–stimulating factor containing supernatant from P3-X63 cells. Medium was exchanged every 48 h, and BMDCs were used after 8–10 days of differentiation to ascertain that ≥80% of the cell population expressed the marker CD11c (43).

Cell stimulation assays

These experiments were performed as previously described (22, 23). RAW 264.7 cells (2.5×10^5) were distributed onto 24-well microplates (JET BIOFIL®, China), and the medium volume was adjusted to 0.5 ml. The plates were incubated for 48 h

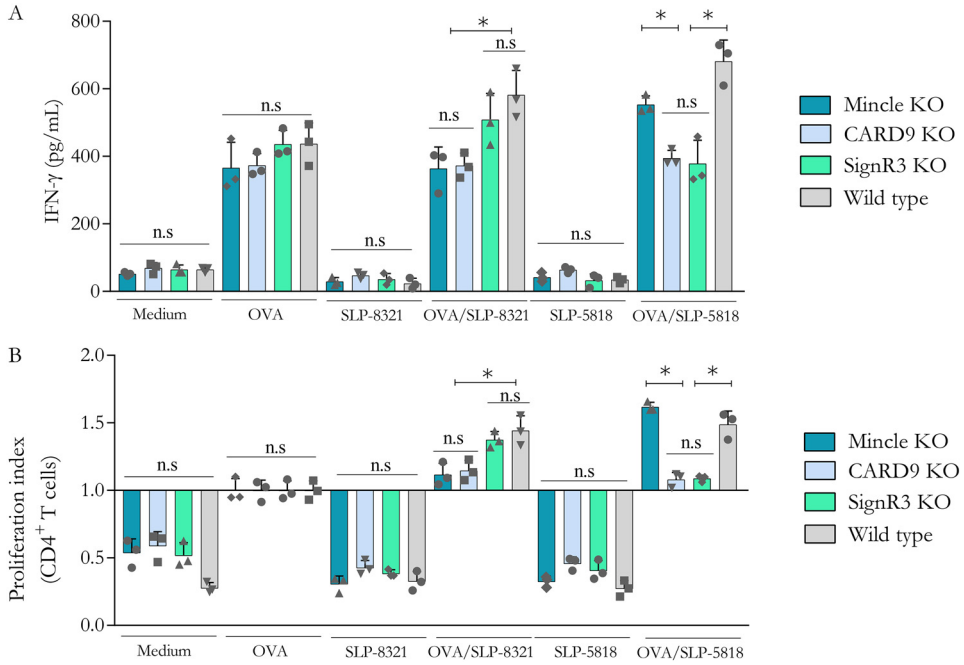

Figure 10. CLR-SLP specific interactions impact on T-cell stimulatory function of the SLP-activated BMDCs. Cells from C57BL/6 and CLR-deficient mice were stimulated with SLP, OVA, or the combination of both for 24 h and then exposed to carboxyfluorescein diacetate succinimidyl ester–labeled CD4+ T cells from OT-II mice using the same experimental model as in Ref. 23. *A*, IFN-γ level in supernatants measured after 5 days. *B*, proliferation index of CD4+ T cells. A representative figure of three independent experiments is shown (±S.D., indicated by *error bars*). *, $P < 0.05$; *n.s.*, not significant; *KO*, knockout.

at 37 °C in a 5% CO_2 95% air atmosphere to allow cell adherence prior to experimentation. After that, the cells were treated with SLP-8321 or SLP-5818 (10 μg/ml), in the presence or absence of LPS 0.1 μg/ml (LPS from *E. coli* O111:B4, Sigma), in Dulbecco's modified Eagle's medium for 24 h at 37 °C in a 5% CO_2 95% air atmosphere. The cells were incubated with anti-CD40 (3/23), and anti-CD86 (P03.1) and then analyzed by flow cytometry.

BMDCs from WT or CLR-deficient mice (1×10^5 cells/well) were distributed onto 96-well microplates (Sarstedt, Germany) and stimulated with SLP-8321 or SLP-5818 (10 μg/ml), LPS (0.25 μg/ml), or the combination of both for 16 h at 37 °C in a 5% CO_2, 95%air atmosphere. Culture supernatants were collected and analyzed by ELISA for IL-6 and tumor necrosis factor α secretion. The cells were incubated with anti-CD16/32 (93) to block cell-surface FcgRII/RIII receptors; stained with anti-CD11c (N418), CD40 (3/23), and CD80 (16-10A1); and then analyzed by flow cytometry.

BMDCs/T cell co-culture assay

Splenocytes were isolated from OT-II transgenic mice by flushing the spleen with complete Iscove's modified Dulbecco's medium. After erythrocyte lysis, the cells were resuspended in magnetic-activated cell separation buffer (0.5% BSA, 2 mM EDTA in PBS). T cells were obtained by magnetic-activated cell separation using Pan T cell isolation kit II, mouse (Miltenyi Biotech, Bergisch Gladbach, Germany) according to the manufacturer's instructions. T cells were labeled with carboxyfluorescein diacetate succinimidyl ester (Sigma–Aldrich) and seeded on a 96-well round bottom culture plate (7×10^4 cells/well). After 30 min, BMDCs treated with OVA (Endo Grade® Ovalbumin, LIONEX GmbH, Germany) or OVA/SLPs were added and incubated for 72 h. Culture supernatants were collected for IFN-γ secretion. Proliferation index of $CD4^+$ T cells within each experimental group was calculated as the ratio between the percentage of $CFSE^{low}$ $CD4^+$ cells and $CFSE^{low}$ $CD4^+$ cells from OVA-treated BMDCs.

Cytokine quantification in culture supernatants

Production of IL-6 by macrophages was analyzed by ELISA from BD-Pharmingen (San Diego). Secretion of IL-6 and TNFα by BMDCs and IFN-γ from purified T cells were analyzed by ELISA from PeproTech. The assays were performed according to the manufacturer's instructions. After determining optical densities, cytokine levels in cell culture supernatants were calculated using the GraphPad Prism 7.0 program.

Immunocytostaining and flow cytometry

After stimulation experiments, the cells were washed twice with PBS containing 2% (v/v) FBS and then labeled with specific monoclonal antibodies for 30 min at 4 °C. The cells were washed twice and then fixed with 1% (v/v) formaldehyde. The cells were analyzed using a FACSCalibur Analyzer (BD Biosciences) or Attune NxT flow cytometer (Thermo Fisher Scientific). Data analysis was performed using the FlowJo Software (FlowJo, Ashland, OR).

Statistical analysis

The values from at least three independent experiments were analyzed by using a one-way or two-way analysis of

variance with Tukey's post hoc test ($p < 0.05$ was considered statistically significant). Statistical analysis was performed with the GraphPad Prism program (GraphPad Software, San Diego, CA).

Data availability

The MS proteomics data have been deposited to the ProteomeXchange Consortium via the PRIDE (44) partner repository with the data set identifier PXD020358.

Author contributions—M. M., G. J. C., A. C. C., B. L., M. d. l. A. S., and A. S. C. formal analysis; M. M. and G. J. C. investigation; M. M., G. J. C. and A. C. C. methodology; M. M., G. J. C. M. d. l. A. S., and A. S. C. writing-original draft; M. M., G. J. C. B. L., M. d. l. A. S., and A. S. C. writing-review and editing; B. L., M. d. l. A. S., and A. S. C. supervision; M. d. l. A. S. and A. S. C. conceptualization; M. d. l. A. S. and A. S. C. funding acquisition.

Funding and additional information—This work was supported by Consejo Nacional de Investigaciones Científicas y Técnicas Grant PIP-11220110100660 (to A. S. C.), Agencia Nacional de Promoción Científica y Tecnológica (ANPCyT) Grants PICT 2013-0736 (to A. S. C.) and PICT 2016-0244 (to M. d. l. A. S.), Universidad de Buenos Aires Grant 20020130100476BA (to A. S. C.), and Universidad Nacional Arturo Jauretche Grant 80020170100031UJ (to M. d. l. A. S.). The Ultraflex II (Bruker) TOF/TOF mass spectrometer was supported by ANPCyT Grant PME 125 (CEQUIBIEM) and the ESI–Orbitrap was supported by ANPCyT Grant PME 2012 (CEQUIBIEM) G. J. C. and M. M. are fellows from ANPCyT and Consejo Nacional de Investigaciones Científicas y Técnicas, respectively. A. S. C. and M. d. l. A. S. are members of Carrera de Investigador Científico y Tecnológico of Consejo Nacional de Investigaciones Científicas y Técnicas. M. M. was also supported by funding from the German Academic Exchange Service (DAAD Deutscher Akademischer Austauschdienst).

Conflict of interest—The authors declare that they have no conflicts of interest with the contents of this article.

Abbreviations—The abbreviations used are: SLP, S-layer glycoprotein; CLR, C-type lectin receptor; HPAEC, high-performance anion-exchange chromatography; HCD, high collision dissociation; WGA, wheat germ agglutinin; ESI, electrospray ionization; BMDC, bone marrow-derived dendritic cell; ANPCyT, Agencia Nacional de Promoción Científica y Tecnológica; CIDCA, Centro de Investigación y Desarrollo en Criotecnología de Alimentos; PNGase F, peptide:*N*-glycosidase F; FBS, fetal bovine serum; IL, interleukin; IFN, interferon; LPS, lipopolysaccharide; PAD, pulse amperometric detector; OVA, ovalbumin; DC-SIGN, dendritic cell–specific intercellular adhesion molecule–3 grabbing non-integrin; ACN, acetonitrile; HILIC, hydrophilic interaction liquid chromatography.

References

1. Messner, P., and Sleytr, U. B. (1992) Crystalline bacterial cell-surface layers. *Adv. Microb. Physiol.* **33,** 213–275 CrossRef Medline
2. Dell, A., Galadari, A., Sastre, F., and Hitchen, P. (2010) Similarities and differences in the glycosylation mechanisms in prokaryotes and eukaryotes. *Int. J. Microbiol.* **2010,** 148178 CrossRef Medline
3. Schäffer, C., and Messner, P. (2017) Emerging facets of prokaryotic glycosylation. *FEMS Microbiol. Rev.* **41,** 49–91 CrossRef Medline
4. Latousakis, D., and Juge, N. (2018) How sweet are our gut beneficial bacteria? A focus on protein glycosylation in *Lactobacillus*. *Int. J. Mol. Sci.* **19,** 136 CrossRef Medline
5. Lavelle, A., and Hill, C. (2019) Gut microbiome in health and disease: emerging diagnostic opportunities. *Gastroenterol. Clin. North Am.* **48,** 221–235 CrossRef Medline
6. Tang, W. H., Kitai, T., and Hazen, S. L. (2017) Gut microbiota in cardiovascular health and disease. *Circ. Res.* **120,** 1183–1196 CrossRef Medline
7. Sára, M., and Sleytr, U. B. (2000) Bacterial S-layers. *J. Bacteriol.* **182,** 859–868 CrossRef Medline
8. Zhu, C., Guo, G., Ma, Q., Zhang, F., Ma, F., Liu, J., Xiao, D., Yang, X., and Sun, M. (2017) Diversity in S-layers. *Prog. Biophys. Mol. Biol.* **123,** 1–15 CrossRef Medline
9. Fagan, R. P., and Fairweather, N. F. (2014) Biogenesis and functions of bacterial S-layers. *Nat. Rev. Microbiol.* **12,** 211–222 CrossRef Medline
10. Gerbino, E., Carasi, P., Mobili, P., Serradell, M. A., and Gómez-Zavaglia, A. (2015) Role of S-layer proteins in bacteria. *World J. Microbiol. Biotechnol.* **31,** 1877–1887 CrossRef Medline
11. Malamud, M., Bolla, P. A., Carasi, P., Gerbino, E., Gómez-Zavaglia, A., Mobili, P., and Serradell, M. A. (2019) S-layer proteins from lactobacilli: biogenesis, structure, functionality and biotechnological applications. In *Lactobacillus Genomics and Metabolic Engineering*, pp. 105–130, Caister Academic Press, Poole, UK
12. Pum, D., and Sleytr, U. B. (2014) Reassembly of S-layer proteins. *Nanotechnology* **25,** 312001 CrossRef Medline
13. Garrote, G. L., Delfederico, L., Bibiloni, R., Abraham, A. G., Pérez, P. F., Semorile, L., and De Antoni, G. L. (2004) Lactobacilli isolated from kefir grains: evidence of S-layer proteins. *J. Dairy Res.* **71,** 222–230 CrossRef Medline
14. Malamud, M., Carasi, P., Bronsoms, S., Trejo, S. A., and Serradell, M. A. (2017) *Lactobacillus kefiri* shows inter-strain variations in the amino acid sequence of the S-layer proteins. *Antonie Van Leeuwenhoek* **110,** 515–530 CrossRef Medline
15. Cavallero, G., Malamud, M., Casabuono, A. G., Serradell, M. A., and Couto, A. S. (2017) A glycoproteomic approach reveals that the S-layer glycoprotein from *Lactobacillus kefiri* CIDCA 83111 is *O*- and *N*-glycosylated. *J. Proteomics* **162,** 20–29 CrossRef Medline
16. Rodrigues-Oliveira, T., Belmok, A., Vasconcellos, D., Schuster, B., and Kyaw, C. M. (2017) Archaeal S-layers: overview and current state of the art. *Front. Microbiol.* **8,** 2597 CrossRef Medline
17. Chinthamani, S., Settem, R. P., Honma, K., Kay, J. G., and Sharma, A. (2017) Macrophage inducible C-type lectin (Mincle) recognizes glycosylated surface (S)-layer of the periodontal pathogen *Tannerella forsythia*. *PLoS One* **12,** e0173394 CrossRef Medline
18. Richards, E., Bouché, L., Panico, M., Arbeloa, A., Vinogradov, E., Morris, H., Wren, B., Logan, S. M., Dell, A., and Fairweather, N. F. (2018) The S-layer protein of a *Clostridium difficile* SLCT-11 strain displays a complex glycan required for normal cell growth and morphology. *J. Biol. Chem.* **293,** 18123–18137 CrossRef Medline
19. Konstantinov, S. R., Smidt, H., de Vos, W. M., Bruijns, S. C., Singh, S. K., Valence, F., Molle, D., Lortal, S., Altermann, E., Klaenhammer, T. R., and van Kooyk, Y. (2008) S layer protein A of *Lactobacillus acidophilus* NCFM regulates immature dendritic cell and T cell functions. *Proc. Natl. Acad. Sci. U.S.A.* **105,** 19474–19479 CrossRef Medline
20. Liu, Z., Ma, Y., Shen, T., Chen, H., Zhou, Y., Zhang, P., Zhang, M., Chu, Z., and Qin, H. (2011) Identification of DC-SIGN as the receptor during the interaction of *Lactobacillus plantarum* CGMCC 1258 and dendritic cells. *World J. Microbiol. Biotechnol.* **27,** 603–611 CrossRef
21. Prado Acosta, M., Palomino, M. M., Allievi, M. C., Sanchez Rivas, C., and Ruzal, S. M. (2008) Murein hydrolase activity in the surface layer of *Lactobacillus acidophilus* ATCC 4356. *Appl. Environ. Microbiol.* **74,** 7824–7827 CrossRef Medline
22. Malamud, M., Carasi, P., Freire, T., and Serradell, M. L. A. (2018) S-layer glycoprotein from Lactobacillus kefiri CIDCA 8348 enhances macrophages response to LPS in a Ca^{+2}-dependent manner. *Biochem. Biophys. Res. Commun.* **495,** 1227–1232 CrossRef Medline

23. Malamud, M., Carasi, P., Assandri, M. H., Freire, T., Lepenies, B., and Serradell, M. L. A. (2019) S-layer glycoprotein from *Lactobacillis kefiri* exerts its immunostimulatory activity through glycan recognition by Mincle. *Front. Immunol.* **10,** 1422 CrossRef Medline
24. Mobili, P., Serradell, M. A., Trejo, S. A., Aviles Puigvert, F. X., Abraham, A. G., and De Antoni, G. L. (2009) Heterogeneity of S-layer proteins from aggregating and non-aggregating *Lactobacillus kefir* strains. *Antonie Van Leeuwenhoek* **95,** 363–372 CrossRef Medline
25. Carasi, P., Ambrosis, N. M., De Antoni, G. L., Bressollier, P., Urdaci, M. C., and Serradell, M. A. (2014) Adhesion properties of potentially probiotic *Lactobacillus kefiri* to gastrointestinal mucus. *J. Dairy Res.* **81,** 16–23 CrossRef Medline
26. Palmisano, G., Melo-Braga, M. N., Engholm-Keller, K., Parker, B. L., and Larsen, M. R. (2012) Chemical deamidation: a common pitfall in large-scale *N*-linked glycoproteomic mass spectrometry-based analyses. *J. Proteome Res.* **11,** 1949–1957 CrossRef Medline
27. del Fresno, C., Iborra, S., Saz-Leal, P., Martínez-López, M., and Sancho, D. (2018) Flexible signaling of myeloid C-type lectin receptors in immunity and inflammation. *Front. Immunol.* **9,** 804 CrossRef Medline
28. Möschl, A., Schäffer, C., Sleytr, U. B., Messner, P., Christian, R., and Schulz, G. (1993) Characterization of the S-layer glycoproteins of two lactobacilli. In *Advances in Bacterial Paracrystalline Surface Layer* pp. 281–284, Springer, Boston, MA
29. Anzengruber, J., Pabst, M., Neumann, L., Sekot, G., Heinl, S., Grabherr, R., Altmann, F., Messner, P., and Schäffer, C. (2014) Protein *O*-glucosylation in *Lactobacillus buchneri*. *Glycoconj. J.* **31,** 117–131 CrossRef Medline
30. Fina Martin, J., Palomino, M. M., Cutine, A. M., Modenutti, C. P., Fernández Do Porto, D. A., Allievi, M. C., Zanini, S. H., Mariño, K. V., Barquero, A. A., and Ruzal, S. M. (2019) Exploring lectin-like activity of the S-layer protein of *Lactobacillus acidophilus* ATCC 4356. *Appl. Microbiol. Biotechnol.* **103,** 4839–4857 CrossRef Medline
31. Messner, P., Steiner, K., Zarschler, K., and Schäffer, C. (2008) S-layer nanoglycobiology of bacteria. *Carbohydr. Res.* **343,** 1934–1951 CrossRef Medline
32. Qazi, O., Hitchen, P., Tissot, B., Panico, M., Morris, H. R., Dell, A., and Fairweather, N. (2009) Mass spectrometric analysis of the S-layer proteins from *Clostridium difficile* demonstrates the absence of glycosylation. *J. Mass Spectrom.* **44,** 368–374 CrossRef Medline
33. Lightfoot, Y. L., Selle, K., Yang, T., Goh, Y. J., Sahay, B., Zadeh, M., Owen, J. L., Colliou, N., Li, E., Johannssen, T., Lepenies, B., Klaenhammer, T. R., and Mohamadzadeh, M. (2015) SIGNR3-dependent immune regulation by *Lactobacillus acidophilus* surface layer protein A in colitis. *EMBO J.* **34,** 881–895 CrossRef Medline
34. Devi, S., Rajakumara, E., and Ahmed, N. (2015) Induction of Mincle by *Helicobacter pylori* and consequent anti-inflammatory signaling denote a bacterial survival strategy. *Sci. Rep.* **5,** 15049 CrossRef Medline
35. Garrote, G. L., Abraham, A. G., and De Antoni, G. L. (2001) Chemical and microbiological characterisation of kefir grains. *J. Dairy Res.* **68,** 639–652 CrossRef Medline
36. Carasi, P., Trejo, F. M., Pérez, P. F., De Antoni, G. L., and Serradell, M. A. (2012) Surface proteins of *Lactobacillus kefir* antagonize *in vitro* cytotoxic effect of *Clostridium difficile* toxins. *Anaerobe* **18,** 135–142 CrossRef Medline
37. Morelle, W., and Michalski, J. C. (2007) Analysis of protein glycosylation by mass spectrometry. *Nat. Protoc.* **2,** 1585–1602 CrossRef Medline
38. Selman, M. H., Hemayatkar, M., Deelder, A. M., and Wuhrer, M. (2011) Cotton HILIC SPE microtips for microscale purification and enrichment of glycans and glycopeptides. *Anal. Chem.* **83,** 2492–2499 CrossRef Medline
39. Mayer, S., Moeller, R., Monteiro, J. T., Ellrott, K., Josenhans, C., and Lepenies, B. (2018) C-type lectin receptor (CLR)–Fc fusion proteins as tools to screen for novel CLR/bacteria interactions: an exemplary study on preselected *Campylobacter jejuni* isolates. *Front. Immunol.* **9,** 213 CrossRef Medline
40. Kostarnoy, A. V., Gancheva, P. G., Lepenies, B., Tukhvatulin, A. I., Dzharullaeva, A. S., Polyakov, N. B., Grumov, D. A., Egorova, D. A., Kulibin, A. Y., Bobrov, M. A., Malolina, E. A., Zykin, P. A., Soloviev, A. I., Riabenko, E., Maltseva, D. V., *et al.* (2017) Receptor Mincle promotes skin allergies and is capable of recognizing cholesterol sulfate. *Proc. Natl. Acad. Sci. U.S.A.* **114,** E2758–E2765 CrossRef Medline
41. Eriksson, M., Johannssen, T., von Smolinski, D., Gruber, A. D., Seeberger, P. H., and Lepenies, B. (2013) The C-type lectin receptor SIGNR3 binds to fungi present in commensal Microbiota and influences immune regulation in experimental colitis. *Front. Immunol.* **4,** 196 CrossRef Medline
42. Heë, R., Storcksdieck Genannt Bonsmann, M., Lapuente, D., Maaske, A., Kirschning, C., Ruland, J., Lepenies, B., Hannaman, D., Tenbusch, M., and Überla, K. (2019) Glycosylation of HIV Env impacts IgG subtype responses to vaccination. *Viruses* **11,** 153 CrossRef Medline
43. Monteiro, J. T., Schön, K., Ebbecke, T., Goethe, R., Ruland, J., Baumgärtner, W., Becker, S. C., and Lepenies, B. (2019) The CARD9-associated C-type lectin, Mincle, recognizes La Crosse virus (LACV) but plays a limited role in early antiviral responses against LACV. *Viruses* **11,** 303 CrossRef Medline
44. Perez-Riverol, Y., Csordas, A., Bai, J., Bernal-Llinares, M., Hewapathirana, S., Kundu, D. J., Inuganti, A., Griss, J., Mayer, G., Eisenacher, M., Pérez, E., Uszkoreit, J., Pfeuffer, J., Sachsenberg, T., Yilmaz, S., *et al.* (2019) The PRIDE database and related tools and resources in 2019: improving support for quantification data. *Nucleic Acids Res.* **47,** D442–D450 CrossRef Medline